

The effects of various spatial distributions of weak noise on rhythmic spiking

Henry C. Tuckwell · Jürgen Jost

Received: 9 February 2010 / Revised: 13 June 2010 / Accepted: 6 July 2010 / Published online: 22 July 2010
© Springer Science+Business Media, LLC 2010

Abstract We consider the response of the classical Hodgkin–Huxley (HH) spatial system in the weak to intermediate noise regime near the bifurcation to repetitive spiking. The deterministic component of the input (signal) is restricted to a small segment near the origin whereas noise, with parameter σ , occurs either only in the signal region or throughout the whole neuron. In both cases small noise inhibits the spiking and there is a minimum in the spike counts at $\sigma \approx 0.15$. At the same value of σ , the variance of the spike counts undergoes a pronounced maximum. For spatially restricted noise, the spike count continues to increase beyond the minimum until $\sigma = 0.5$, but in the case of spatially extended noise the spike count begins to decline around $\sigma = 0.35$ to give a local maximum. For both spatial distributions of noise, the variance of the spike count is found to also have a local minimum at about $\sigma = 0.4$. Examples are given of the probability distributions of the spike counts and the spatial distributions of spikes with varying noise level. The differences in behaviours of the spike counts as noise increases beyond 0.3 are attributable to noise-induced spiking outside the signal region, which has a larger probability of occurrence when the noise is over an extended region. This aspect is investigated by ascertaining the probability of noise-induced spiking as a function of noise level and examination of the corresponding latency distributions. These findings prompt a definition of weak noise in the

standard HH model as that for which the probability of secondary phenomena is negligible, which occurs when σ is less than about 0.3. Finally, if signal and weak ($\sigma < 0.3$) noise are applied on disjoint intervals, then the noise has no effect on the instigation or propagation of spikes, no matter how large its region of application. These results are expected to apply to type 2 neurons in general, including the majority of cortical pyramidal cells.

Keywords Stochastic model · Rhythmic firing · Spatial model neuron

1 Introduction

Many recent theoretical and experimental studies have been concerned with the inhibitory effect of weak noise on neuronal spiking (Tuckwell 2005; Paydarfar et al. 2006; Ozer and Graham 2008; Ozer and Uzuntarla 2008). Such observations are related to the general phenomena of stimulus-induced cessation of firing (Forger and Paydarfar 2004; Calitoui et al. 2008). More recently, studies of the HH-system of ordinary differential equations, called a point model neuron, with stochastic input have revealed new and interesting phenomena. In particular, at mean input current densities near the critical value for repetitive firing, it was found that weak noise could strongly inhibit spiking and that there was a pronounced minimum in the firing rate as the noise level increased from zero (Tuckwell et al. 2009).

Whereas the point HH model has been the subject of a large number of studies and analyses, both with and without noise, as for example in Hassard (1978), Yu and Lewis (1989), Brown et al. (1999), Tiesinga et al. (2000),

Action Editor: Bard Ermentrout

H. C. Tuckwell (✉) · J. Jost
Max Planck Institute for Mathematics in the Sciences,
Inselstr 22., 04103 Leipzig, Germany
e-mail: tuckwell@mis.mpg.de

Tuckwell and Wan (2005), Lv (2007), Bruce (2007), Torcini et al. (2007), and Tuckwell and Jost (2009), there have been relatively few articles on the spatial system (e.g., Horikawa 1991; Faisal and Laughlin 2007).

It is thus of interest to see how the spatial HH-system responds to weak noise, where in addition there exist many possibilities for the spatial distributions of the deterministic component of the input (signal) and of the noise. It is found that with weak noise the spatial HH system exhibits much more complex behavior than the point model. Preliminary investigations for this system showed that the spatial system shared some of the properties of the space-clamped model, but that the degree of overlap of noise and signal was an important factor (Tuckwell and Jost 2010). In this article we report on an extended analysis of this system. The HH system is employed with one space dimension, which is most accurate for a nerve cylinder, usually considered to be of uniform diameter. This simple geometry can nevertheless be used to gain some insight into the properties of neurons with complex anatomy by appealing to the mapping from a neuronal branching structure to a cylinder (Rall 1962; Walsh and Tuckwell 1985), thus reducing the multi-segment problem to one of solving a cable equation in one space dimension. Provided certain constraints are met, the resulting cylinder has a uniform diameter as is assumed in our preliminary investigations below. Investigations of the effects of changing diameters, as for example at some dendritic or telodendritic branch points, are not addressed here.

2 Description of model

The spatial Hodgkin–Huxley system (Hodgkin and Huxley 1952) consists of the cable partial differential equation for nerve membrane voltage

$$C_m \frac{\partial V}{\partial t} = \frac{a}{2R_i} \frac{\partial^2 V}{\partial x^2} + \bar{g}_K n^4 (V_K - V) + \bar{g}_{Na} m^3 h (V_{Na} - V) + g_l (V_l - V) + I(x, t)$$

and differential equations for m, h, n describing the sodium and potassium conductances. Thus

$$\frac{\partial m}{\partial t} = \alpha_m(V)(1 - m) - \beta_m(V)m$$

with similar equations for n and h . Initial and boundary conditions must of course be specified. The quantities $C_m, \bar{g}_K, \bar{g}_{Na}, g_l$, and $I(x, t)$ are respectively the membrane capacitance, maximal potassium conductance, maximal sodium conductance, leak conductance and

applied current density for unit area (1 cm^2). R_i is the intracellular resistivity, a is the fiber radius, all times are in ms, all voltages are in mV, all conductances per unit area are in mS cm^{-2} , R_i is in $\Omega \text{ cm}$, C_m is in $\mu\text{F cm}^{-2}$, distances are in cm, and current density is in $\mu\text{A cm}^{-2}$. $n(x, t), m(x, t)$ and $h(x, t)$ are the potassium activation, sodium activation and sodium inactivation variables. Their evolution is determined by the voltage-dependent coefficients, the α s and β s which are given in the Appendix. The following standard parameter values are used throughout: $a = 0.0238$, $R_i = 34.5$, $\bar{g}_K = 36$, $C_m = 1$, $\bar{g}_K = 36$, $\bar{g}_{Na} = 120$, $g_l = 0.3$, $V_K = -12$, $V_{Na} = 115$ and $V_l = 10$. For the initial values, $V(x, 0) = 0$, the resting level, and for the auxiliary variables the equilibrium resting values are used, for example $n(x, 0) = \alpha_n(0)/(\alpha_n(0) + \beta_n(0))$. The boundary conditions were set as zero-derivative at both end points.

The above system is considered with applied currents (consisting of “signal” plus noise) of the following form

$$I(x, t) = \mu(x, t) + \sigma(x, t)w(x, t)$$

on subsets of a cylindrical nerve cell extending from $x = 0$ to $x = L$. The functions $\mu(x, t)$ and $\sigma(x, t)$ are deterministic and specify the spatial (and temporal) distributions of the mean and variance of the noisy input. The deterministic component of the input, $\mu(x, t)$ takes the form

$$\mu(x, t) = \mu > 0, \quad 0 < x < x_1 < L, \quad t > 0,$$

and $\mu(x, t) = 0$, otherwise. In the stochastic component, $\{w(x, t), x \in [0, L], t \geq 0\}$ is a two-parameter white noise with covariance function

$$\text{Cov}[w(x, s), w(y, t)] = \delta(x - y)\delta(t - s).$$

The spatial distribution of noise is set to

$$\sigma(x, t) = \sigma > 0, \quad 0 < x_2 < x < x_3 \leq L, \quad t > 0,$$

and $\sigma(x, t) = 0$, otherwise. The numerical integration of the stochastic system is performed by discretization using an explicit method, shown to be accurate by comparison with analytical results in similar systems (Tuckwell 2008).

3 Effects of various spatial distributions of noise

3.1 Rhythmic firing with steady applied current and no noise

Consider the spatial HH-system with a constant current applied indefinitely over a (small) region near the origin, for example extending from $x = 0$ to $x_1 = 0.2$, and

with a total length set at $L = 6$. When the stimulus μ is greater than some critical value, there ensues a train of regularly spaced spikes, corresponding to repetitive (periodic) firing in the HH-system of ODE's. In order to quantify the spiking activity, the number $N(T)$ of spikes at time T on $(0, L)$ is employed. There is a sudden increase in the value of $N(T)$ as μ increases through a critical value, which depends on x_1 , paralleling the appearance of a limit cycle solution in the ODE system. Such dependence of $N(T)$ on μ was explored for two values of x_1 , viz 0.1 and 0.2, and gave critical values of μ at about 6.5 and 6.0, respectively. In consideration of the behavior of the HH system of ODE's with noise, it was then of interest to examine the effects of noise on the spike counts near the bifurcation points for the PDE case.

3.2 An illustrative example

In Fig. 1 are shown examples of the effects of noise with the following parameters: $\mu = 6.7$, $x_1 = 0.1$, $x_2 = 0$, and $x_3 = L = 6$. That is, the noise component is σ on the whole interval $(0, L)$. In the top record there is no noise and there are 9 spikes. In the middle two records, with a noise level of $\sigma = 0.1$ there is a significant diminution of the spiking activity, with only 1 spike in one case and 3 in the other. With the noise turned up to $\sigma = 0.3$ (bottom record) the number of spikes is greater, but

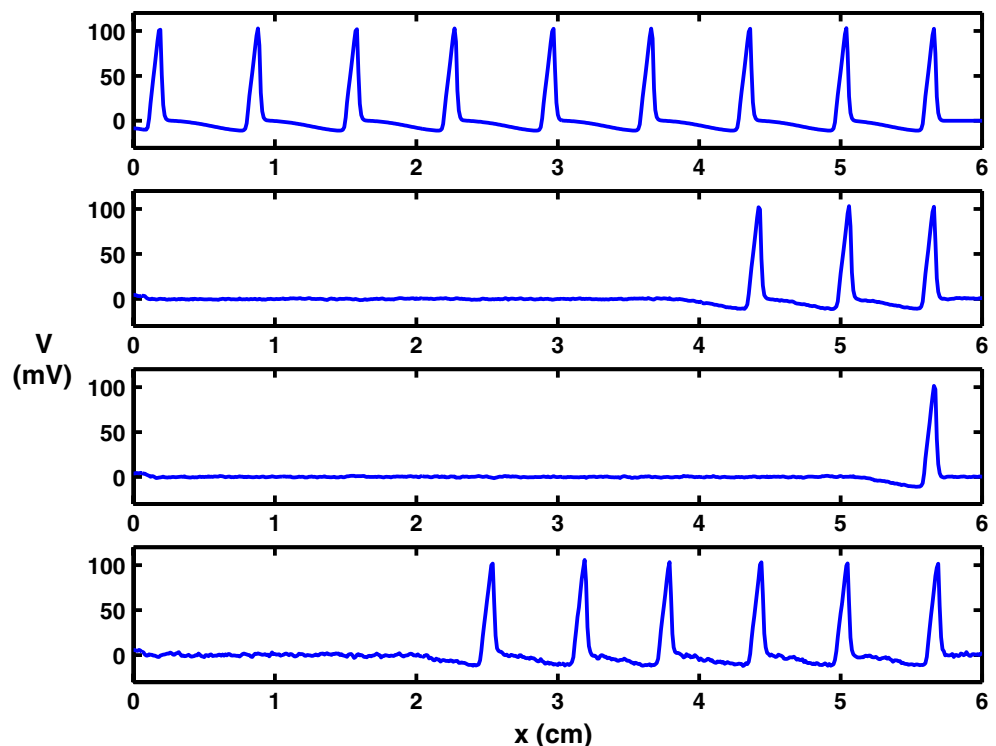
still less than in the noise-free case, there being 6 in the example shown.

3.3 Noise throughout the cable length

Spike counts were obtained with a signal extending to $x_1 = 0.1$ on a cable of total length $L = 3$. The speed of the action potentials is such that by $t = 80$ the first spike generated near the origin has travelled to nearly the right-hand point ($x = 3$), so simulations were performed until this value of t . Values of σ ranged from 0 to 0.5, somewhat larger than in our previous investigation. The value of x_3 was set to be the cable length $L = 3$, so with $x_2 = 0$ there was noise of the same amplitude uniformly on the whole neuron. The number of trials for each point in the following is 250, which is five times as many as in our previous report.

Figure 2 gives mean spike counts $E[N]$ and Fig. 3 gives corresponding standard deviations σ_N as functions of noise level. The left panel in Fig. 2 shows plots of mean spike counts $E[N]$ versus noise level for the three values of μ . 95% confidence limits are also indicated. For $\mu = 5$ (green curve), the introduction of weak noise begins to take effect when $\sigma = 0.1$, as the mean spike count starts to increase. Beyond this value of σ , the mean spike count steadily increases until about $\sigma = 0.4$, after which value the spike rate declines. The latter decline was not observed previously

Fig. 1 Showing examples of the inhibitory effects of noise on regular spiking in the spatial HH system for a mean current density near the bifurcation to repetitive spiking. Here V is plotted against x at $t = 160$ ms. In the top record there is no noise ($\sigma = 0$), in the second and third records, relatively small noise of amplitude $\sigma = 0.1$, and in the bottom record, a larger noise of amplitude $\sigma = 0.3$. For parameter values, see text



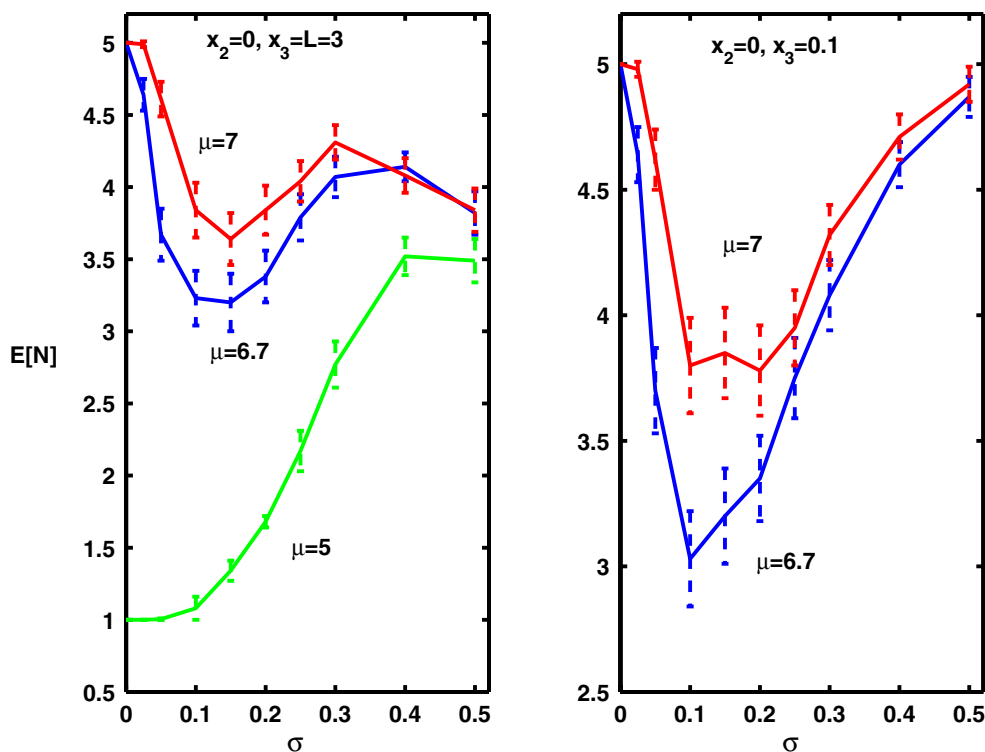


Fig. 2 Showing the effects of increasing noise on mean numbers $E[N]$ of spikes as a function of noise level. 95% confidence limits are shown for the mean (250 trials). The deterministic component of the input current is of strength μ on the small interval from $x = 0$ to $x = 0.1$. *Left panel:* Noise of strength σ is applied throughout the neuron. Results for three values of the signal strength μ . The *bottom curve* is for a value of μ well

below the critical value at which repetitive firing occurs, whereas the *upper two curves*, where minima and then maxima occur, are for μ near the bifurcation point. *Right panel:* Noise is only applied over the same region as the signal ($0 < x < 0.1$) for two values of the signal strength μ . For both values of μ pronounced minima occur as the noise amplitude increases but there are no subsequent maxima

because no values of σ greater than 0.3 were employed. The standard deviation σ_N of N increases steadily from $\sigma_N = 0.06$ at $\sigma = 0.05$ to a maximum (for the values used) $\sigma_N = 1.27$ at $\sigma = 0.3$ and is somewhat less than this for $\sigma > 0.3$.

With $\mu = 6.7$ (blue curve), a value at which periodic spiking occurs without noise, increasing weak noise results in a sharp drop in mean spike count with a pronounced minimum at $\sigma = 0.15$. Increasing noise level then sharply increases $E[N]$ until a maximum occurs around $\sigma = 0.3$, which was the largest value of σ in our previous report (Tuckwell and Jost 2010). The standard deviation σ_N here increases to reach a maximum of 1.55 at $\sigma = 0.15$ where the mean has a minimum. Beyond that value of σ , σ_N declines slowly to reach a minimum of 0.84 when $\sigma = 0.4$ and increases again by $\sigma = 0.5$.

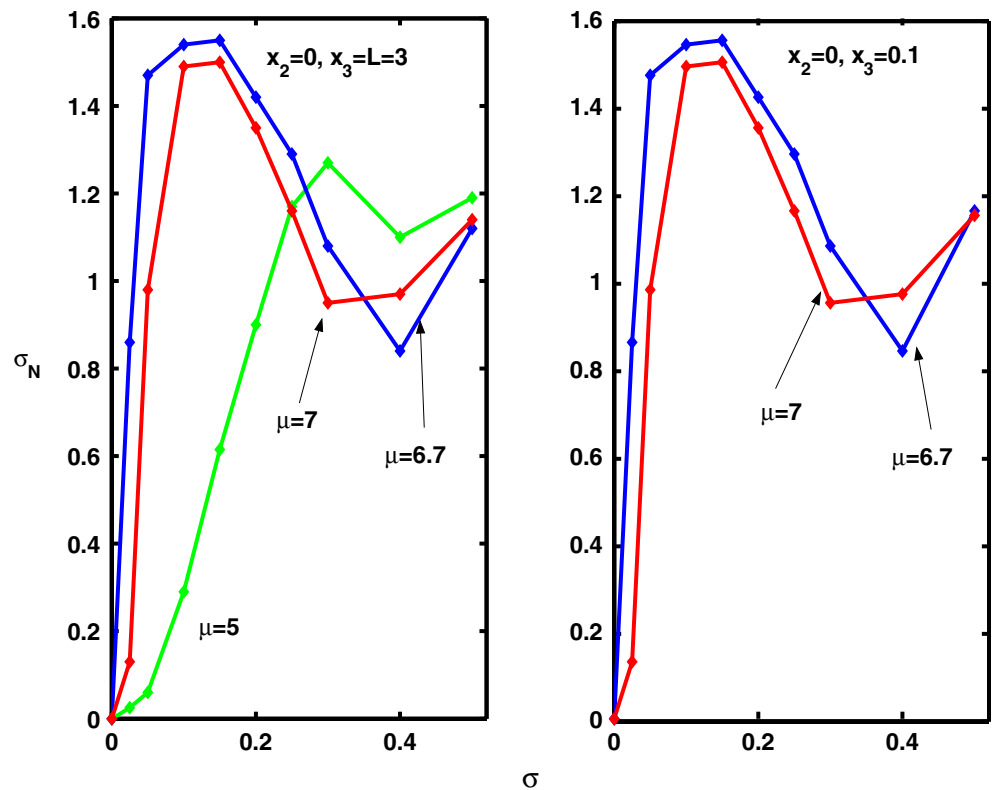
For the last value of μ considered, $\mu = 7$ (blue curve), which is further above the threshold for repetitive activity, the dependence of mean spike count on σ mimics that for $\mu = 6.7$, but that the spike rates are higher and the minimum, which occurs at a slightly

larger value of $\sigma \approx 0.15$, is shallower. For $\sigma > 0.3$, $E[N]$ decreases and actually is less than the value for $\mu = 6.7$ when $\sigma = 0.4$, but approximate equality occurs at $\sigma = 0.5$. The standard deviation of N displays similar behaviour to that for $\mu = 6.7$. It is interesting to observe that for $\mu = 6.7$ and $\mu = 7$, the maximum variance of the spike counts occurs when the mean spike count is a minimum (see below).

3.4 Noise restricted to a small region around the signal

It was originally thought that noise over the whole length of the neuron would have a stronger inhibitory effect on spiking than noise over a small region. It turns out that this is not the case for weak noise but it is partially true for stronger noise. In the right-hand panels of Figs. 2 and 3 are shown the mean and standard deviations of spike counts obtained when the noise is restricted to the signal region, $0 < x < x_1 = x_3 = 0.1$. Considering first the means, their dependence on noise amplitude σ is about the same for values of σ up to

Fig. 3 The standard deviations of the spike counts whose means are given in the previous figure. *Left panel:* Noise of strength σ is applied throughout the neuron. Results for three values of the signal strength μ . *Right panel:* Noise is only applied over the same region as the signal ($0 < x < 0.1$) for two values of the signal strength μ



about 0.3. However, for $\sigma > 0.3$ the mean spike counts when $x_3 = 0.1$ keep climbing with increasing σ and do not exhibit the maxima seen in the left panel. It is interesting to again observe that for $\mu = 6.7$ and $\mu = 7$, the maximum variance of the spike counts occurs when the mean spike count is a minimum. With a larger region of excitation (signal) so that $x_1 = 0.2$, spike counts (not shown here) were similarly obtained with various noise amplitudes for values of $\mu = 5, 6.2$ and 6.5 . Again, the first of these values is less than the critical value for repetitive firing and the other two close to or just above the critical value. The behaviours of the spike counts were similar to those for $x_1 = 0.1$.

3.5 Distributions of spike counts and spatial distributions

In addition to the first two moments of the spike counts, we show in Fig. 4 examples of the actual (discrete) probability distributions of $N(T)$. In all cases $\mu = 6.7$. The left column gives distributions for noise on the whole interval ($0 < x < L = 3$) whereas in the right column are results for noise restricted to $(0, 0.1)$. All these distributions are based on 250 trials and in all cases the signal is on the small region from 0 to $x_1 = 0.1$. In the noise-free case (not shown), the frequency distribution is the single value 250 concentrated at 5 spikes.

It can be seen that for small noise, $\sigma = 0.05$, both for noise everywhere and noise restricted to the small region, the full complement of 5 spikes survived the noise in about 50% of trials and that in the remaining trials there were roughly equal chances of 1,2,3 or 4 spikes. For $\sigma = 0.15$, near the minima in expected spike counts, the full complement of 5 spikes survived the noise in only about 33% of trials and there is a greater chance of only 1 or 2 spikes than 3 or 4. The distribution of $N(T)$ here is very approximately uniform on $\{1, 2, 3, 4, 5\}$. At the somewhat larger noise level, $\sigma = 0.3$, the distribution of $N(T)$, which looks roughly negative geometric, becomes more concentrated at 4 and 5 with only about a 25% chance of less than 4 spikes. When the noise is at the largest value considered, $\sigma = 0.5$, the distributions of $N(T)$ are radically different between not only the cases of spatially restricted and unrestricted noise, but also from the cases with smaller noise. For $x_3 = L$, there are no instances with just 1 spike and the probability is highest of 3 or 4 spikes with a small chance, about 10%, of extra spikes (6 or 7). With noise spatially restricted so that $x_3 = 0.1$, there are no occurrences of either 1 or 2 spikes, and it is very likely (75% chance) that there will be 5 spikes as in the noise-free case. There is also about a 10% chance of one extra spike.

Fig. 4 The frequency of spike counts N corresponding to several data points in Fig. 2 for a mean signal strength $\mu = 6.7$. The number of trials in each case is 250. In the *left column* the noise occurs throughout the whole neuron whereas in the *right column* it occurs only in the signal region. For both columns, significant changes in the shapes of the distributions occur as the noise increases. For the largest noise considered, $\sigma = 0.5$, very different distributions of spike counts are obtained in the restricted (*right column*) and unrestricted (*left column*) noise cases

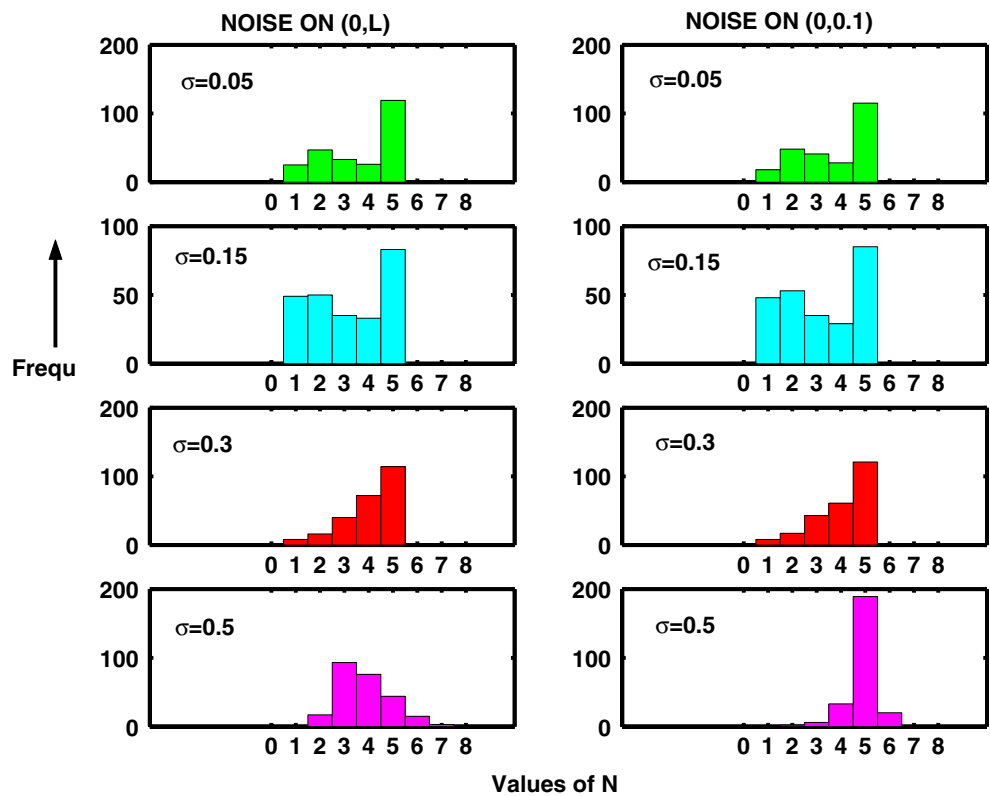
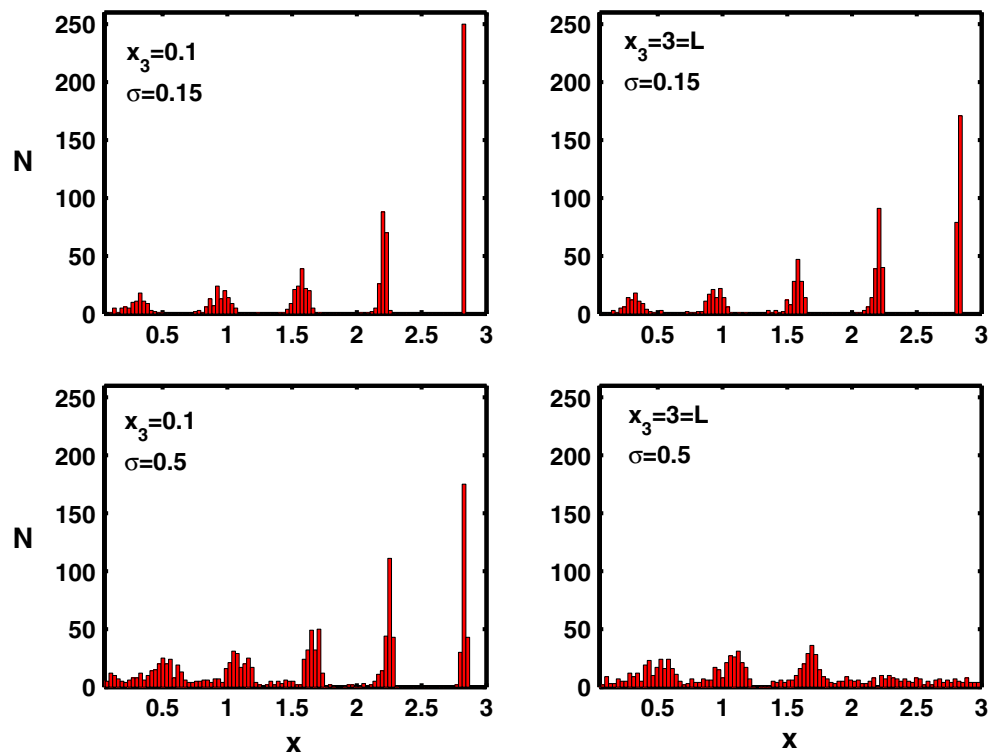


Fig. 5 The spatial distributions of spikes at $t = 80$ ms corresponding to several data points in Fig. 2 (250 trials). In all cases $\mu = 6.7$. In the *left column* noise is restricted to the signal region and in the *right column*, noise occurs throughout the whole neuron. If there were no noise then the distributions would have counts of 250 at each of five regularly spaced positions. Traces of the latter are easily seen in all except the *bottom right graph* where strong ubiquitous noise has destroyed the regularity of the spike train



It is also of interest to examine the spatial patterns of spikes, 4 illustrative cases of such results being shown in Fig. 5 for $\mu = 6.7$. When there is no noise, these distributions are 5 regularly spaced counts of 250, with spatial separations of about 0.6. In the top left panel, for small noise on a small interval, there is no disturbance for the first spike (counting from the right) as all 250 are in the same position. In the second spike position there are about 190 spikes, with a little variability in position. Only 129 spikes are in the third position, 110 in the fourth position and 87 in the 5th position, with increasing variability. For the same noise level on the whole length of the neuron, as seen in the top right panel, there are about the same numbers of spikes in each position, but there is somewhat more scatter in their positions. For example, there is even a little variability in the position of the first spike. In the lower left panel, where the noise is large at $\sigma = 0.5$, but only on a small interval (to $x = 0.1$), the 250 first spikes have somewhat more scatter. The later spikes show considerable variability in position so it is not really clear which spikes are in 4th or 5th position. Finally, for $\sigma = 0.5$ on the whole length, the scatter of all spikes is so large it is not possible to associate a spike position with a rank position. The reasons for this will be elaborated on in the next subsection.

4 Interference due to secondary phenomena

It had been noted that in some trials, with large σ , *secondary phenomena* were observed (Horikawa 1991; Faisal and Laughlin 2007; Tuckwell 2008; Tuckwell and Jost 2010) in which noise-induced pairs of spikes emerged outside the signal region and interfered with the train emitted from the signal region. In the simple geometry considered above, such secondary phenomena readily explain the differences between weak and strong noise and strong noise on small and large intervals. To understand quantitatively these effects, we considered stimulation with noise only, such that $\mu(x, t) = 0$. This is especially useful in order to clarify the definition of weak noise. Figures 6 and 7 show two interesting features of the results of such simulations (250 trials) for two spatial distributions of noise: on the whole length, $0 < x < L = 3$, and restricted to a small segment, $0.1 < x < 0.3$.

In Fig. 6 the probability that any noise-induced spike arose is plotted against noise level. When the noise is on the whole length, the chance of a spike is negligible for σ less than about 0.3 and rises to 0.5 at $\sigma = 0.4$ and to 1 by $\sigma = 0.5$. When the noise is restricted to (0.1, 0.3),

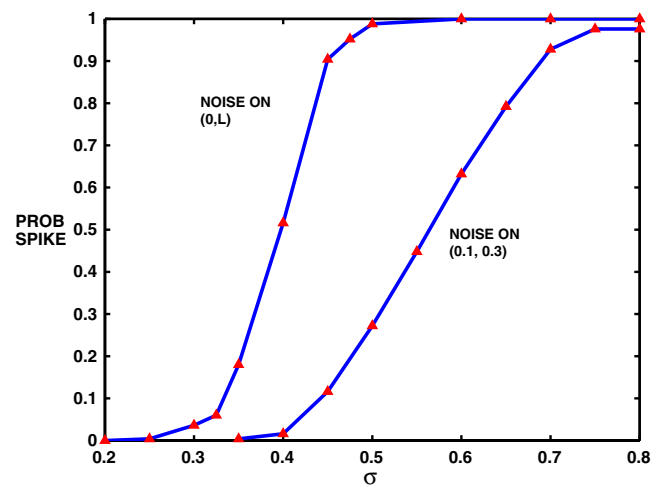
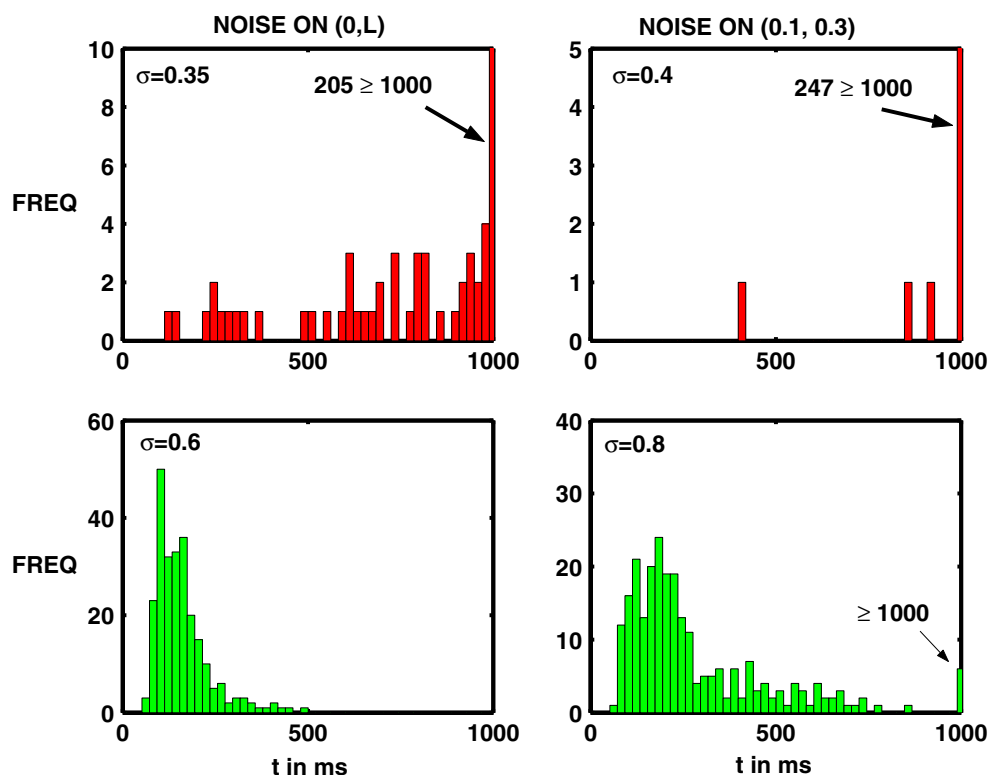


Fig. 6 The probability, as a function of noise level σ , of noise-only induced spiking ($\mu = 0$) for noise on the whole length of the cell (*left-most curve*) and for noise restricted to a small interval of length 0.2 (*right-hand curve*). In all trials the simulation was terminated at 1,000 ms, so these probabilities are conditional but almost absolute as can be seen from the latency distributions given in the following figure. 250 trials at each data point

the chance of a spike is negligible for σ less than about 0.4 and rises to 0.5 at about $\sigma = 0.6$ and to nearly 1 by $\sigma = 0.8$. These properties assist in understanding the difference between the results for spike counts in the left and right parts of Fig. 2. In the case of spatially restricted noise, the chances of interference with the spike train emitted from the signal region are negligible so the results (right-hand graph) resemble those for the HH point model. On the other hand, for noise along the whole length there are significant probabilities of spontaneous spiking when $\sigma \geq 0.3$, which explains why in fact the spike count starts to decrease at such noise levels. This also explains the increases in variance of the spike counts at large σ in both parts of Fig. 3.

Figure 7 shows the latency distributions for spiking corresponding to 4 of the data points in Fig. 6. The trials were terminated at 1,000 ms, so that trials with no spike until that time are ascribed a latency of 1,000 ms in the histograms. For noise on (0, L), with $\sigma = 0.35$, about 80% of trials resulted in a noise-induced spike before 1,000 ms, and 100% with $\sigma = 0.6$. In contrast, with noise on (0.1, 0.3), there are hardly any spikes in the first 1,000 ms when $\sigma = 0.4$, but when $\sigma = 0.8$ nearly all trials saw spikes arise before 1,000 ms. Such waiting-time distributions afford additional insight into the different results obtained in the cases of weak versus strong noise and the cases of spatially restricted and spatially unrestricted noise.

Fig. 7 The latency distributions for spiking corresponding to the four sets of results in the previous figure. In the *upper two plots* where the noise is relatively weak, a large fraction of the 250 trials did not result in a spike in the first 1,000 ms. In the *left-hand lower plot*, with stronger noise along the whole neuron, all trials gave spikes before 1,000 ms



5 Dependence upon overlap of signal and noise regions in the case of weak noise

It is of interest to see how varying the extent of the noise around the signal region affects the propagation of action potentials. It was at first surprising to find that, with $x_1 = 0.1$, $x_2 = 0.1$ and $x_3 = 0.2$, when there was weak noise just to the right of the excitatory stimulus, no reduction in spike count occurred. Thus, it seemed that weak noise at the source of the spiking could cause a significant reduction in spike count, but noise with the same magnitude and extent over a region disjoint from the region of excitation, tended to have little or no effect on spike propagation. In a systematic investigation, with the mean excitation fixed at $\mu = 6.2$ for $0 < x < 0.2$, noise of strength $\sigma = 0.1$ was applied for $x_2 < x < x_3$ where $x_3 - x_2$ was fixed at 0.2 and x_2 varied from 0, corresponding to complete overlap, to 0.2, corresponding to zero overlap.

From histograms of spike counts (50 trials), the fraction of trials on which there was interference of the spike train by weak noise was obtained. The results, which are shown in Table 1, provide a clear demonstration of the significance of the degree of overlap of (weak) noise and signal. For example, with complete overlap ($x_2 = 0$, $x_3 = 0.2$) there were 11 of 50 trials with a full complement of 9 spikes as in the noise-free

case, representing interference, mainly in the form of inhibition, by noise in 78% of trials. In contrast, with $x_2 = 0.12$ and $x_3 = 0.32$, giving 40% overlap, there were 9 spikes in all 50 trials, indicating zero interference. The probability of interference (as a %) versus degree of overlap is given in the second column of the table. This probability is seen to remain at zero until the overlap is 40% and then increases monotonically to achieve the value near 80% when the overlap is complete. In the third column of Table 1 are also given the mean spike counts $E[N]$. The mean spike count remains at 9 until the overlap is greater than 40%. These results illustrate dramatically the importance of overlap of signal and weak noise, defined here as $\sigma < 0.3$, for the latter to

Table 1 Weak noise interference with rhythmic spiking

Overlap (%)	Interference (%)	$E[N]$
0	0	9
20	0	9
40	0	9
45	4	8.9
50	12	8.7
55	25	8.5
60	48	6.5
80	74	5.3
100	78	4.9

have an inhibitory effect on spiking. That is, a spike may traverse a region of weak noise, but if the same noise is applied at the source of the spike, there is a considerable chance of a reduction or cessation of spiking.

6 Discussion

In previous related articles (see Tuckwell et al. 2009) we have explored the effects of weak noise on rhythmic firing in the point Hodgkin–Huxley model. The main results concerned the inhibition of spiking by weak noise and the occurrence of a minimum in the mean spike count as the noise level increased from zero when the mean input is near the critical value for sustained firing.

Such observations are related to the general phenomena of stimulus-induced cessation of firing (Forger and Paydarfar 2004; Calitoui et al. 2008) and noise-induced delays in firing in single HH neurons with periodic input current (Pankratova et al. 2005) or networks of such neurons (Ozer and Graham 2008; Ozer and Uzuntarla 2008). The inhibitory effect of noise on rhythmic firing has been explained in transitions from one attractor, a limit cycle, to another, being a stable rest point (Tuckwell et al. 2009; Tuckwell and Jost 2009). The inhibitory effect of noise on spiking has been graphically experimentally demonstrated in the squid axon (Paydarfar et al. 2006). The occurrence of minima with increasing noise level may be referred to as *inverse stochastic resonance* as it has a character opposite to the maxima associated with stochastic resonance (McDonnell and Abbott 2007).

We had noted in a preliminary report (Tuckwell and Jost 2010) that similar but more complex phenomena occur in the HH PDE (cable) system when the mean input is near the critical value for sustained firing. In the present article we have explored these effects in more detail with more extensive simulations and increased noise level beyond the weak noise regime. In fact, the definition of weak noise in the spatial HH system is possible in terms of the probabilities of occurrence of noise-induced spiking (see Fig. 6). The mode of failure of spiking at weak noise levels is similar in principle to that in the point model as the voltage paths (now in space and time) in cases of failure are close to those for the repetitive spike train until just before the 2nd or 3rd etc spike is about to form, whereupon the trajectory wanders on a path away from threshold. Consequently, the spike train terminates prematurely as the system thereafter stays at low levels of depolarization, preventing the possibility of further spikes.

We have examined not only the means of the spike counts N as functions of noise level but also their variances, probability distributions and spatial distributions. An important observation was that the variance of N has a pronounced maximum at about the same values of σ that the mean has a minimum. The probability distributions of N at such noise levels are almost uniform (see Fig. 4). In addition, a local minimum in the variance was found for larger noise levels as shown in Fig. 3. However, the mean spike count shows different behaviour depending on the spatial extent of the noise. As seen in Fig. 2, when noise is restricted to a small region, and in particular coinciding with the location of the signal, $E[N]$ increases monotonically as σ increases from about 0.1–0.15 to 0.5. However, when the noise has large spatial extent, and in particular embraces the signal region, there is also a maximum in $E[N]$ at $\sigma \approx 0.35$. The decline in spike count beyond the weak noise regime is readily explained by interference with the signal-induced spikes and their annihilation by pairs of noise-induced spikes. The important role of the spatial overlap of signal and noise in the case of weak noise has also been noted.

The spatial Hodgkin–Huxley equations belong to the class of reaction-diffusion systems (see e.g. Smoller 1983; Jost 2007). The mathematical theory of stochastic nonlinear stochastic PDE's of the type we are concerned with is abstract and there is a paucity of results concerning traveling wave solutions (spikes) in the presence of noise. It is possible that although there is no standard bifurcation analysis for the HH PDE system, some insight could be obtained from general theory (Kielhöfer 2003; Haragus and Iooss 2010). This analysis will not be carried out here, but it is likely that many of the properties of the system of ODEs apply, in some sense, to the PDEs.

In order to obtain some insight into the phenomena just described, we distinguish, in the case of noise throughout the whole cylinder, the small region $0 < x < x_1$ where an external current is applied and where consequently the spikes are generated, and the larger region $x_1 < x < L$ where no such current is applied and where the spike is propagated. The first region was found to be much more sensitive to perturbations than the second. The typical nonlinear effects are generated by the interaction of the nonlinear reaction term and the linear diffusion term. In the first regime, where the spike is generated, the reaction terms dominate the behavior. Therefore, the effects of perturbations are similar to those in the non-spatial Hodgkin–Huxley equations which constitute a system of nonlinear ordinary differential equations. In particular, noise when applied at a particular part of the periodic trajectory

that corresponds to the regular spiking can destroy an incipient spike (Tuckwell et al. 2009). The second regime is modelled as a travelling wave solution of the Hodgkin–Huxley equation, whose existence has been investigated in (Hastings 1976). According to the analysis of Conley (1975), this has the consequence that the fast reaction dynamics corresponding to the propagated spike branches off from the vicinity of an equilibrium set at positions that are different from the original rest state $V = 0$. Therefore, the region at the incipient spike where the solution slowly traverses a narrow region of its basin of attraction, as analyzed in Tuckwell and Jost (2009), is avoided. Consequently, the travelling wave is much less sensitive to perturbations than the spike generation.

In summary, there are new effects in the spatial HH system that cannot arise in the ODE system and which clearly demonstrate the utility of spatial models as providing more realistic insights into the behavior of real neurons. Future work on these complex phenomena involving noise is needed for the elucidation of their role, not just in the relatively simple HH model, but in more realistic models of central nervous system neurons such as, for example, in Destexhe et al. (1998), Rhodes and Llinás (2005) and Komendantov et al. (2007).

Appendix: The coefficients in the auxiliary equations

$$\alpha_n(V) = \frac{10 - V}{100[e^{(10-V)/10} - 1]}$$

$$\beta_n(V) = \frac{1}{8}e^{-V/80}$$

$$\alpha_m(V) = \frac{25 - V}{10[e^{(25-V)/10} - 1]}$$

$$\beta_m(V) = 4e^{-V/18}$$

$$\alpha_h(V) = \frac{7}{100}e^{-V/20}$$

$$\beta_h(V) = \frac{1}{e^{(30-V)/10} + 1}$$

Acknowledgement Thanks to Olivier Faugeras for some useful references.

References

- Brown, D., Feng, J., & Feerick, S. (1999). Variability of firing of Hodgkin–Huxley and FitzHugh–Nagumo neurons with stochastic synaptic input. *Physical Review Letters*, *82*, 4731–4734.
- Bruce, I. C. (2007). Implementation issues in approximate methods for stochastic Hodgkin–Huxley models. *Annals of Biomedical Engineering*, *35*, 315–318.
- Calitoui, D., Oommen, B. J., & Nussbaum, D. (2008). Spikes annihilation in the Hodgkin–Huxley neuron. *Biological Cybernetics*, *98*, 239–257.
- Conley, C. (1975). On travelling wave solutions of nonlinear diffusion equations. *Springer Lecture Notes in Mathematics*, *38*, 498–510.
- Destexhe, A., Neubig, M., Ulrich, D., & Huguenard, J. (1998). Dendritic low-threshold calcium currents in thalamic relay cells. *Journal of Neuroscience*, *18*, 3574–3588.
- Faisal, A. A., & Laughlin, S. B. (2007). Stochastic simulations on the reliability of action potential propagation in thin axons. *P.L.o.S. Computational Biology*, *3*, e79.
- Forger, D. B., & Paydarfar, D. (2004). Starting, stopping, and resetting biological oscillators: In search of optimum perturbations. *Journal of Theoretical Biology*, *230*, 521–532.
- Haragus, M., & Iooss, G. (2010). *Local bifurcations, center manifolds, and normal forms in infinite dimensional dynamical systems*. Berlin: Springer.
- Hassard, B. (1978). Bifurcation of periodic solutions of the Hodgkin–Huxley model for the squid giant axon. *Journal of Theoretical Biology*, *71*, 401–420.
- Hastings, S. P. (1976). On travelling wave solutions of the Hodgkin–Huxley equations. *Archive for Rational Mechanics and Analysis*, *60*, 229–257.
- Hodgkin, A. L., & Huxley, A. F. (1952). A quantitative description of membrane current and its application to conduction and excitation in nerve. *Journal of Physiology*, *117*, 500–544.
- Horikawa, Y. (1991). Noise effects on spike propagation in the stochastic Hodgkin–Huxley models. *Biological Cybernetics*, *66*, 19–25.
- Jost, J. (2007). *Partial differential equations* (2nd ed.). Berlin: Springer.
- Kielhöfer, H. (2003). *Bifurcation theory: An introduction with applications to P.D.E.s*. Berlin: Springer.
- Komendantov, A. O., Trayanova, N. A., & Tasker, J. G. (2007). Somato-dendritic mechanisms underlying the electrophysiological properties of hypothalamic magnocellular neuroendocrine cells: A multicompartmental model study. *Journal of Computational Neuroscience*, *23*, 143–168.
- Lv, Y. G. (2007). Theoretical evaluation on monitoring hypothermic anesthesia by the electrical response of human skin neurons. *Forschung im Ingenieurwesen*, *71*, 79–88.
- McDonnell, M. D., & Abbott, D. (2007). What is stochastic resonance? Definitions, misconceptions, debates, and its relevance to biology. *P.L.o.S. Computational Biology*, *5*, e1000348.
- Ozer, M., & Graham, L. J. (2008). Impact of network activity on noise delayed spiking for a Hodgkin–Huxley model. *European Physical Journal B*, *61*, 499–503.
- Ozer, M., & Uzuntarla, M. (2008). Effects of the network structure and coupling strength on the noise-induced response delay of a neuronal network. *Physics Letters A*, *372*, 4603–4609.
- Pankratova, E. V., Polovinkin, A. V., & Mosekilde, E. (2005). Resonant activation in a stochastic Hodgkin–Huxley model: Interplay between noise and suprathreshold driving effects. *European Physical Journal B*, *45*, 391–397.
- Paydarfar, D., Forger, D. B., & Clay, J. R. (2006). Noisy inputs and the induction of on-off switching behavior in a neuronal pacemaker. *Journal of Neurophysiology*, *96*, 3338–3348.

- Rall, W. (1962). Theory of physiological properties of dendrites. *Annals of the New York Academy of Sciences*, 96, 1071–1092.
- Rhodes, P. A., & Llinás, R. (2005). A model of thalamocortical relay cells. *Journal of Physiology*, 565, 765–781.
- Smoller, J. (1983). *Shock waves and reaction-diffusion equations*. Berlin: Springer.
- Tiesinga, P. H. E., José, J. V., & Sejnowski, T. J. (2000). Comparison of current-driven and conductance-driven neocortical model neurons with Hodgkin–Huxley voltage-gated channels. *Physical Review E*, 62, 8413–8419.
- Torcini, A., Luccioli, S., & Kreuz, T. (2007). Coherent response of the Hodgkin–Huxley neuron in the high-input regime. *Neurocomputing*, 70, 1943–1948.
- Tuckwell, H. C. (2005). Spike trains in a stochastic Hodgkin–Huxley system. *BioSystems*, 80, 25–36.
- Tuckwell, H. C. (2008). Analytical and simulation results for the stochastic spatial Fitzhugh–Nagumo neuron. *Neural Computation*, 20, 3003–3035.
- Tuckwell, H. C., & Jost, J. (2009). Moment analysis of the Hodgkin–Huxley system with additive noise. *Physica A*, 388, 4115–4125.
- Tuckwell, H. C., & Jost, J. (2010). Weak noise in neurons may powerfully inhibit the generation of repetitive spiking but not its propagation. *P.L.o.S. Computational Biology*, 6, e1000794.
- Tuckwell, H. C., Jost, J., & Gutkin, B. S. (2009). Inhibition and modulation of rhythmic neuronal spiking by noise. *Physical Review E*, 80, 031907.
- Tuckwell, H. C., & Wan, F. Y. M. (2005). Time to first spike in stochastic Hodgkin–Huxley systems. *Physica A*, 351, 427–438.
- Walsh, J. B., & Tuckwell, H. C. (1985). Determination of the electrical potential over dendritic trees by mapping onto a nerve cylinder. *Journal of Theoretical Neurobiology*, 4, 27–46.
- Yu, X., & Lewis, E. R. (1989). Studies with spike initiators: Linearization by noise allows continuous signal modulation in neural networks. *IEEE Transactions on Biomedical Engineering*, 36, 36–43.